Rayleigh scattering correlation spectroscopy on diffusion dynamics of nanoparticles under intense laser irradiation

Ping-Yu Hee[a], Takayuki Uwada*[b], Kazunori Okano[a], Atsushi Miura[a], Hiroshi Masuhara*[a]

[a]Department of Applied Chemistry and Institute of Molecular Science, National Chiao Tung University, Hsinchu 30010, Taiwan;
[b]Department of Chemistry, Josai University, Sakado, 350-0295, Japan

ABSTRACT

Rayleigh scattering correlation microspectroscopy is developed and applied to study diffusion dynamics of some nanospheres in water. It was clearly found that the diffusion constant of gold nanoparticles decreased with increasing excitation laser power at the excitation wavelength of higher absorption cross section. This behavior was explained in terms of a coupling between laser trapping by the scattering excitation laser itself and laser heating of the particle. In the case of non-absorbing nanospheres such as silica and polystyrene, the excitation power dependence can be ascribed only to the laser trapping. Experimental setup is introduced, theoretical formulation is described, and future development of this measurement is considered.

Keywords: Rayleigh scattering, correlation spectroscopy, gold nanoparticles, photothermal heating, laser trapping

1. INTRODUCTION

When laser light is tightly focused close to the diffraction limit by using high numerical aperture lens, photon momentum transfer results in formation of three dimensional trapping potential, exerting photon pressure on small targets. Utilizing the photon force, optical tweezers methods have been developed and laser trapping phenomena have been elucidated[1]. In the past few decades, a tremendous amounts of papers have been published on trapping and manipulating micrometer-sized objects from polymer particle to biological applications[2,3]. Recently, the target of the photon pressure is expanding towards nanomaterial and small molecules[3]. When the photon pressure potential is sufficiently larger than the thermal energy of the nanomaterials, they can be trapped stably at the focus. The depth of the photon pressure potential is determined by polarizability of the trapped material and laser power. The polarizability of such nanomaterial is roughly linear to the volume, so that combination of intense laser light with a high numerical aperture lens becomes more essential for nanomaterial to overcome the thermal energy. In this size region, a number of nanomaterials can be trapped in a single

*Emails; uwada@josai.ac.jp (TU), masuhara@masuhara.jp (HM)
Phone +81-049-271-7996, Fax +81-049-271-7985 (TU)
Phone +886-3-571-2121 ext. 56593, Fax +886-3-571-2121 ext. 56593 (HM)

Optical Trapping and Optical Micromanipulation X, edited by Kishan Dholakia, Gabriel C. Spalding,
Proc. of SPIE Vol. 8810, 88102T · © 2013 SPIE · CCC code: 0277-786X/13/$18 · doi: 10.1117/12.2023022

Downloaded From: http://proceedings.spiedigitallibrary.org/ on 04/27/2014 Terms of Use: http://spiedl.org/terms

focal point simultaneously, because the laser spot is much larger than nanometer scale. Interestingly, the trapped nanomaterials can be assembled in the focal point, which indicates that photon pressure can modify an electrostatic interaction among nanomaterials in the focal point. Our group has reported some applications of this photon pressure to assembling of nanomaterial such as metallic nanoparticles[4], latex nanoparticles[5], polymers[6,7,8,9], molecular J-aggregates[10], and so on. Recently our group achieved photon pressure-induced crystallization and crystal growth of amino acids in solution[11,12,13], which clearly shows further potential application of photon pressure.

Despite development of the photon pressure application to nanomaterial/small molecule assembling and crystallization, the dynamic processes of the optical assembly in real space have been rarely considered due to the lack of mature methods for studying the diffusion properties in such microscopic region. Although spectroscopic detection of nanoparticles aggregation at the trapping laser focus were performed[4,14,15,16], the quantitative analysis of the dynamic sequence from suppression of Brownian motion of the nanoparticles to simultaneous trapping of a number of the particles, leading to assembling based on diffusion constant, was not studied sufficiently. On the other hand, optical fluctuation spectroscopy under an optical microscope can be an alternative tool to elucidate the diffusion property of nanoparticles in a small volume. The progress of stabilized laser and highly-sensitive photodetector enables us to obtain the time fluctuation in the observed signal of the particles induced by laser irradiation, which directly gives information on Brownian motion of the particles. Therefore, the analysis of the fluctuation in the time domain with autocorrelation function (ACF) or in the frequency domain by Fourier transform provides the size, shape, and environment, as well as the structure and internal dynamics. The most widespread ones in the optical fluctuation spectroscopy are classified according to the signal, namely, dynamic light scattering (DLS)[17] and fluorescence correlation spectroscopy (FCS).[18,19,20]

In past decade, FCS has been employed to study dynamics under the photon pressure. Hosokawa et al. have clearly show that the association dynamics of the fluorescent nanoparticles with 24 nm diameter confined in an optical trapping potential by using microscopic FCS method[5,21]. Their quantitative analysis of ACFs as a function of trapping laser power revealed that the laser trapping dynamics of nanoparticles can be divided into two phenomena, simultaneous and numerous trapping of the particles and clustering of the particles, depending on the concentration of the particles in the trapping laser focal spot. Ito et al. measured ACFs of small fluorescent molecules in solution and estimated local temperature elevation in the solution accompanying laser trapping based on the hydrodynamic analysis[22]. As demonstrated by them, FCS is capable of studying molecular/nanomaterials dynamic process of the optical assembly, however, there is a critical limitation that sample should show strong emission though most materials do not show fluorescence. From viewpoint of the expanding the target sample of investigation to non-fluorescent materials, it is necessary to establish methodology based on DLS.

In this study, we built a Rayleigh scattering correlation microspectroscopy system, which enables us to measure ACF based on the intensity fluctuation of Rayleigh (elastic) scattering at different wavelength under an optical microscope with a confocal setup, and studied ACF of nanospheres suspension in water as a function of input laser power for Rayleigh

Downloaded From: http://proceedings.spiedigitallibrary.org/ on 04/27/2014 Terms of Use: http://spiedl.org/terms

scattering excitation. Because Rayleigh scattering is proportional to the input light intensity and to 6th power of the radius of the sample particles, it is in principle possible to obtain signal from any target as increasing the laser input power. This should be an advantage compared with fluorescence-based technique, however, such intense laser input also might disturb hydrodynamics of target, especially high-absorbing material. To examine the laser trapping dynamics of molecules/nanomaterials based on DLS technique, elucidating the effect of the Rayleigh scattering excitation is required. In this presentation we report experimental system and theoretical formulation, and analyze and consider diffusion dynamics of several nanoparticles under laser trapping.

2. EXPERIMENT

Gold nanospheres (diameter: 0.1 μm. Gold: EMGC100, BBI.) were dispersed in pure water with the concentration 1×10^9 particles/ml. After sonication for 10 minutes, the colloidal solution was contained in a perfusion chamber (diameter: 1 cm, depth: 2 mm, CoverWell, Electron Microscopy Science) settled on a cover glass slide and was used as a sample. For comparison, samples of silica or polystyrene nanospheres (Silica: 24041-10, Polyscience. Polystyrene: 00876-15, Polyscience.) dispersed in pure water were also prepared in a same manner.

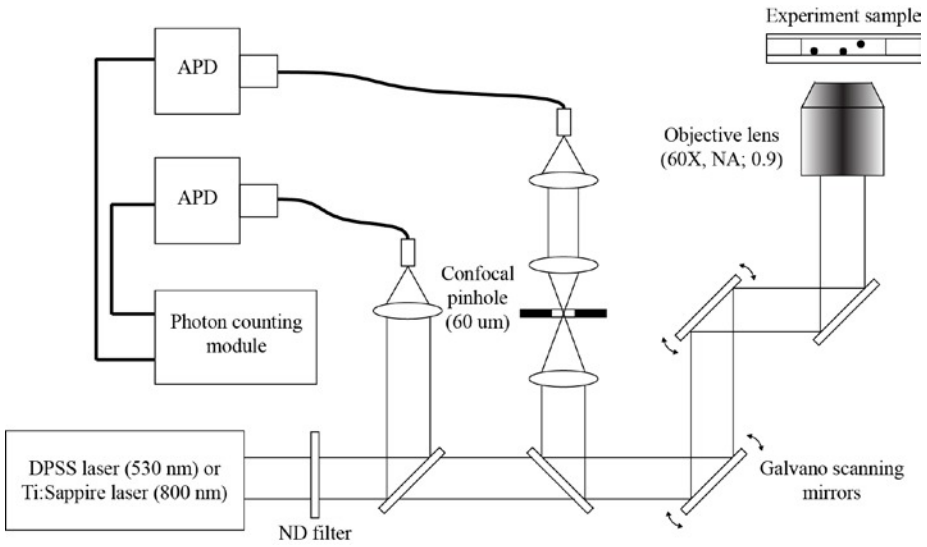

Figure 1. A schematic illustration of the instrumental setup.

Figure 1 illustrates our Rayleigh scattering correlation microspectroscopy system. Laser beam from a diode-pumped solid state (DPSS) laser (wavelength, 532 nm) and a Ti:Sapphire laser (wavelength, 800 nm; Tsunami, Spectra-Physics) with CW mode are employed as light sources for the correlation spectroscopy. The laser light is introduced to an inverted confocal laser-scanning microscope (FV300 and IX-71, Olympus). The objective lens (magnification, 60; NA., 0.9; UPLSAPO, Olympus) focuses the light beam to the sample and collects its back-scattered light signal at the same time. The signal was introduced to a confocal pinhole (60 μm) and passed to a light detector via an optical fiber. The input laser

Downloaded From: http://proceedings.spiedigitallibrary.org/ on 04/27/2014 Terms of Use: http://spiedl.org/terms

power to sample is measured before the objective lens. We used an avalanche photodiode (APD) (PCD100, Newport) connected to a photon-counting device (High Resolution Timing Module, Newport) to record Rayleigh scattering light intensity fluctuation in the time domain. Another APD was used to monitor the fluctuation in the intensity of input laser light.

3. RESULTS AND DISCUSSION

A representative scattered light intensity fluctuation from gold nanosphere suspension with 10 μW excitation at 532 nm is shown in Fig. 2 (a). The spike-like signal is due to Rayleigh scattering from a nanoparticle, which crosses the laser focus volume within short time. In this study, this intensity fluctuation in time domain is analyzed by autocorrelation function that generates an ACF curve $G_{diff}(\tau)$, which visualizes diffusion motion of particles in solution based on following equation[17,18].

$$G_{diff}(\tau) = \frac{\langle \delta I(\tau)\delta I(0)\rangle}{\langle I(0)\rangle^2} = 1 + \frac{1}{N}\cdot\frac{1}{\left(1+\frac{\tau}{\tau_D}\right)}\cdot\frac{1}{\sqrt{1+\frac{k^2\cdot\tau}{\tau_D}}} \quad (1)$$

where N is an average number of particles in an effective focal volume. The focal volume at the focus of a Gaussian laser

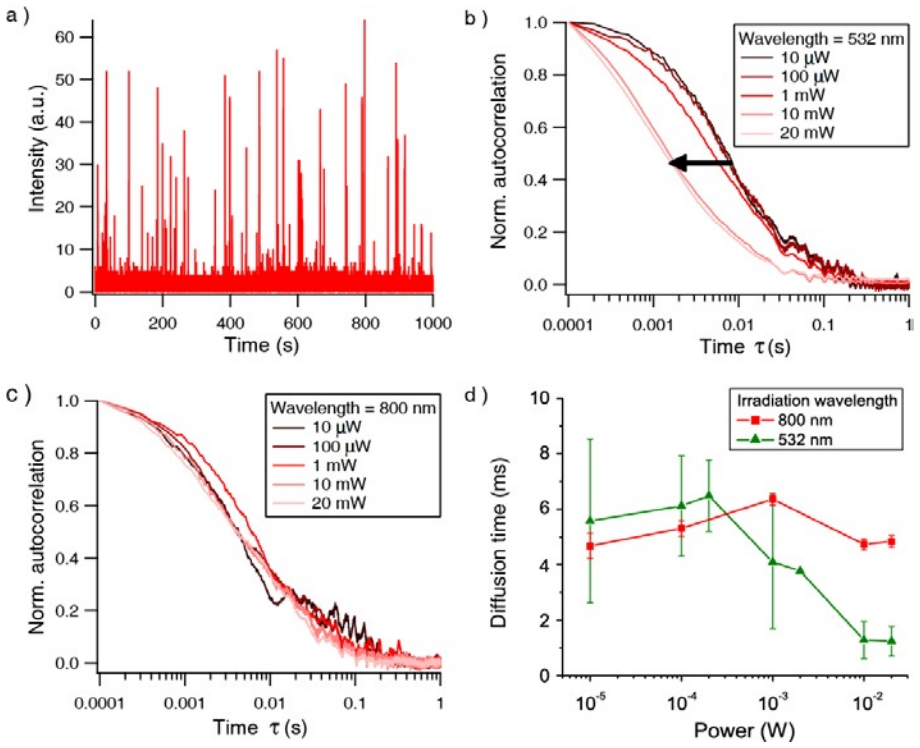

Figure 2 a) Temporal profile of scattering intensity of 100-nm-sized gold nanosphere under 10 μW irradiation at 532 nm. b, c) The ACF under various irradiation power at 532 nm and 800 nm, respectively. d) The plot of diffusion time obtained by fitting ACF with Eq. 1.

Downloaded From: http://proceedings.spiedigitallibrary.org/ on 04/27/2014 Terms of Use: http://spiedl.org/terms

beam is assumed to be ellipsoid-shaped. Here *k* is defined as the ratio between diameter ω_0 and length z_0 of the focal volume. Diffusion time, τ_D, is obtained by analytical fitting of a ACF curve to Eq. 1, is expressed as

$$\tau_D = \frac{\omega_0^2}{8D} = \frac{3\pi\eta a\omega_0^2}{4k_B T} \tag{2}$$

where D denotes diffusion constant of the particles. ω_0, η, a, and T corresponds to the laser beam radius, viscosity of solvent, the particle radius, and temperature, respectively.

On the basis of this analysis for the signal fluctuation, the ACF curves of gold nanosphere suspension irradiated at 532 nm and 800 nm with ranging from 10 μW to 20 mW are obtained and shown in Fig. 2(b) and (c). Under 532 nm irradiation, it is shown that the ACF of gold nanospheres shifted to the short-delay-time side with increasing the laser power. Because the shorter decay of the ACF leads to the decrease of the diffusion time as shown in eq. (1), so that this behavior implies that diffusion speed increased with the increase in laser power.

On the other hand, under 800 nm irradiation, the ACFs of gold nanospheres did not show large increase in diffusion time when irradiation power increased. The diffusion time constant τ_D of gold nanosphere was obtained as a function of the irradiation power at 532 nm and 800 nm by the curve fitting of the ACFs and summarized in Fig. 2 (d). Because of the difference of the geometric factor *k* in eq. (1) which depends on the size of the focal spot (k = 0.189 and 0.126 for the detection wavelength at 532 nm and 800 nm, respectively, based on our optical setup), the diffusion time is in principle larger at 532 nm excitation as seen in the lower power range. However, above milli watt order, the diffusion time at 532 nm became smaller than that at 800 nm, and the difference gradually became larger with increasing the input power. Eventually, we found that gold nanosphere diffusion time constant increased up to 4 times when laser intensity increased at 532 nm.

Downloaded From: http://proceedings.spiedigitallibrary.org/ on 04/27/2014 Terms of Use: http://spiedl.org/terms

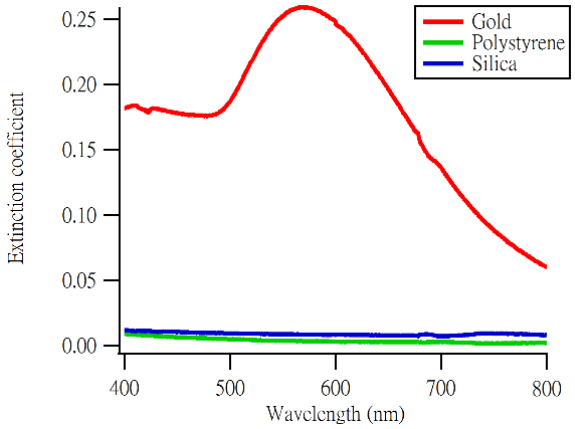

Figure 3. Extinction spectra of the gold, polystyrene and silica nanospheres used in this study. Sample is measured by UV-vis. absorption spectroscopy. The concentration of the colloidal solution was ca. 5.5×10^9 particle/ml.

In principle, observation in the optical fluctuation spectroscopy does not depend on the excitation wavelength and power. However, in this case, we suppose that the laser excitation itself affected the hydrodynamics of the particle with depending on the laser wavelength and power. To establish the DLS technique under an optical microscope, the mechanism should be examined and clarified. Possible mechanism is originated from highly light absorption and scattering in gold nanospheres. As shown in Figure 3, gold nanospheres with the diameter of 100 nm exhibits strong extinction in visible region especially around 550 nm. In spherical particles, they show resonance band of free electron oscillation upon electric field of incident light around 550 nm, which is called as localized surface plasmon resonance (LSPR) band. Therefore, scattering and absorption cross sections, C_{sca} and C_{abs}, respectively, are larger around the resonance band compared with out of the resonance band. It should be noted here that the extinction spectrum shows sum of C_{sca} and C_{abs}, thus (extinction spectrum) $\propto C_{sca}+C_{abs}$. At first, let us consider the effect of the scattering/absorption force driving on the particle. Theoretically, when photon pressure is exerted on nanomaterials, i.e., Rayleigh particles that are smaller than the wavelength of laser light, the time-averaged total force acting on the trapped particles can be written as follows[23,24];

$$F = \frac{1}{2}\varepsilon_m \alpha \nabla \mathbf{E}^2 + \frac{n_m \langle \mathbf{E} \times \mathbf{B} \rangle (C_{scat} + C_{abs})}{c} \quad (3)$$

where $\boldsymbol{E}$ and $\boldsymbol{B}$ denote the electric field and magnetic flux density, respectively, and ∇ represents a gradient with respect to the spatial coordinates. ε_m, n_m, C_{scat}, C_{abs}, and c represent the permittivity of the surrounding medium, its refractive index, light scattering and absorption cross section of the particle, and speed of light in vacuum, respectively. The polarizability of the particle, α, under the dipole approximation is given by

Downloaded From: http://proceedings.spiedigitallibrary.org/ on 04/27/2014 Terms of Use: http://spiedl.org/terms

$$\alpha = 4\pi r^3 \frac{\left(\frac{n_p}{n_m}\right)^2 - 1}{\left(\frac{n_p}{n_m}\right)^2 + 2} \tag{4}$$

where r, and n_p are the radius of the particle and the refractive index of the particle, respectively. The gradient force of photon pressure is described as the first term of eq. (3). The scattering/absorption force to the particle, which is given in the second term of eq. (3), is derived from the change in the direction of the Poynting vector of the electromagnetic wave. As expressed in eq. (3), the gradient force is proportional to the gradient of light intensity and points in the direction of the intensity gradient, while the scattering force is proportional to the Poynting vector and the direction is along the beam direction. Thus the gradient force can trap the particle at the focal spot but scattering/absorption force may disturb stable trapping.

Time averaged trapping and scattering/absorption force energy are summarized as below.

$$U_{trap} = \frac{1}{2}\varepsilon_m \alpha \mathbf{E}^2, \quad U_{sca+abs} = \frac{n_m \mathbf{E}^2 (C_{sca} + C_{abs})}{c}\omega \tag{5}$$

where ω denotes frequency of the input light. For stable laser trapping, the potential energy of laser trapping, U_{trap}, should overcome the sum of the scattering/absorption energy, $U_{sca+abs}$, and thermal energy of the particle, k_BT, as shown below

$$U_{trap} > U_{sca+abs} + k_B T \tag{6}$$

While k_BT can be normally neglected, the diffusion time of the particles in suspension under the photon pressure, τ_D', is expressed by modification of eq. (2) as follows[5];

$$\tau_D' = \tau_D + \left(\frac{U_{trap} - U_{sca+abs}}{k_B T}\right)\tau_D \tag{7}$$

where τ_D is the diffusion time without the photon pressure in the field. This equation implies that the diffusion time increase with the trapping potential energy, however, the scattering and absorption energies disturb it.

As shown in eq. (5), the energies U_{trap} and $U_{sca+abs}$ are proportional to electric field-squared $\boldsymbol{E}^2$. In polar coordinate system, the electric filed $\boldsymbol{E}(r,z)$ is connected to the light intensity distribution $I(r,z)$ as follows[23,24];

$$I = \frac{n_m \varepsilon_0 c}{2}\left|\mathbf{E}\right|^2 \tag{8}$$

The light intensity distribution of a focused light around the focus $I(r,z)$ is expressed in the Gaussian-Lorentzian form as follows;

$$I(r,z) = \frac{2P}{\pi \omega_0^{\,2}} \exp\left(-\frac{2r^2}{\omega_0^{\,2}}\right) \tag{9}$$

Downloaded From: http://proceedings.spiedigitallibrary.org/ on 04/27/2014 Terms of Use: http://spiedl.org/terms

where P and ω_0 denote laser power and beam radius at the waist in lateral, respectively. At trapping wavelength λ=532 nm and numerical aperture of objective lens NA=0.9, we determined ω_0 as 680 nm. At the center of the focal spot, r=0, then we can calculate energies in eq. (5).

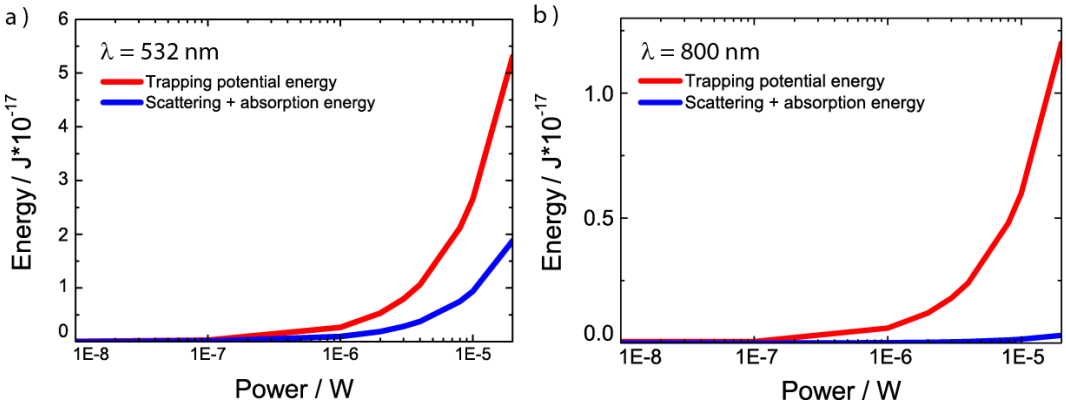

Figure 4. The calculated optical potential for gold nanospheres in the trap a) at 532 nm and b) 800 nm. Trapping potential is larger than 3 times of the sum of scattering and absorption potential at 532 nm and is larger than 40 times of the sum at 800 nm.

The comparison between calculated U_{trap} and $U_{sca+abs}$ as a function of the incident laser power based on eq. (5) is shown in Figure 4, where trapping potential is larger than 3 times of the sum of scattering and absorption potential at 532 nm and is larger than 40 times of the sum at 800 nm. As parameters, the complex refractive indices of gold at 532 and 800 nm are taken from a literature by Johnson[25]. The scattering and absorption cross sections of a gold nanoparticle with 100 nm-diameter embedded in a medium whose refractive index are calculated on the basis of Mie theory. Refractive index of the medium is set to 1.33. The other parameters are chosen from the experimental condition. As shown in Fig. 4, both of the trapping potential and scattering/absorption energies increases super linearly with the input power. The amount of the energy in the trapping potential is always higher than that of absorption/scattering energy, indicating the gold nanoparticles can be trapped at the focus. The values of the trapping potential energy is always larger at 532 nm input, resulting from the higher polarizability. On the other hand, the ratio between U_{trap} and $U_{sca+abs}$ can be explained in terms of the difference of absorption and scattering cross section of a gold nanoparticles at 532 and 800 nm. This simulation clearly suggests that the effect of the incident laser on scattering and absorption force is critical near the LSPR wavelength and the diffusion time, τ_D', would be much more modified by them compared to the case at 800 nm excitation according to eq. (7), while the trapping force is also strong at 532 nm. We consider that this estimation is consistent with the experimental result.

Downloaded From: http://proceedings.spiedigitallibrary.org/ on 04/27/2014 Terms of Use: http://spiedl.org/terms

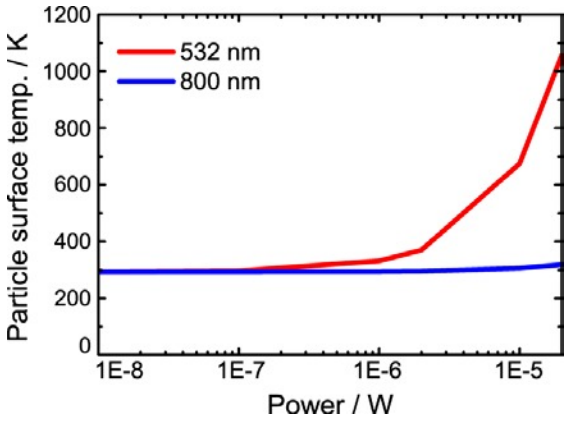

Figure 5. The calculated surface temperature of gold nanosphere as a function of irradiation power at 532 and 800 nm.

Secondly, temperature elevation of the particle medium induced by laser heating by the excitation laser should be considered[26]. Because the metallic nanoparticle such as gold absorbs and scatters light energy efficiently around LSPR band, the part of the absorbed energy can be converted to heat, resulting in temperature elevation of the particle[27]. Then the heat is consequently transferred to the surroundings, so called as the photo-thermal effect. Under this circumstance, temperature change around gold nanosphere will be significant. From eq. (2), it can be predicted that the diffusion motion becomes vigorous upon higher laser intensity input leading to temperature elevation in the particle medium. At steady state, temperature elevation around the laser-heated particle as a function of r, distance from the center of the particle, is formulated as follows[27];

$$T(r,\infty) - T_{\infty} = \frac{\left(\frac{dQ}{dT}\right)}{4\pi r\kappa} \tag{10}$$

where Q, κ denotes absorbed energy by a particle and thermal conductivity of water. dQ/dt can be connected to the absorption cross section of the particle, C_{abs}, and input laser power by using eq (9) as follows.

$$\frac{dQ}{dt} = I \cdot C_{abs} = \frac{P}{\pi\left(\frac{\omega_0}{2}\right)^2} \cdot C_{abs} \tag{11}$$

According to eq. (11), the steady-state temperature of a gold nanoparticle at the surface (r=a) as a function of the laser power is calculated and summarized in Figure 5. The C_{abs} value of the 100-nm-diameter gold nanparticle is calculated based on Mie theory. It is obvious that the temperature of gold elevates quite drastically at 532 nm excitation, whereas that at 800 nm excitation is almost constant. The generated heat in the particle by laser excitation is of course transferred to the surrounding and disturbs the particle motion via eq. (2), resulting in the shorter diffusion time. In addition, the high temperature also affects the stability of the laser trapping, as shown in eq. (6). Consequently, we conclude that a coupling between the laser trapping and the laser heating induced by the excitation of DLS can modify the ACF curves and this is

Downloaded From: http://proceedings.spiedigitallibrary.org/ on 04/27/2014 Terms of Use: http://spiedl.org/terms

quite dependent on the scattering and absorption cross sections, which varies with the wavelength. Because the DLS measurement itself can affect ACF curve if the particle exhibit strong scattering/absorption, the careful data treatment is required in such case.

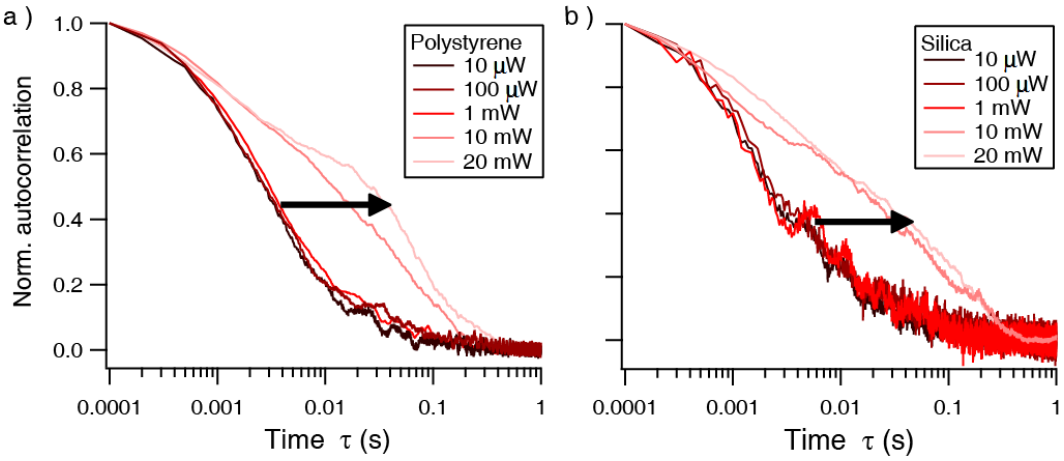

Figure 6. ACF of a) polystyrene and b) silica nanosphere solution showing irradiation power-dependence at 532 nm.

In order to clarify this assumption concerning the coupling of laser trapping and laser heating under DLS measurement, we then examined the irradiation power-dependence of the diffusion motion for polystyrene and silica nanospheres as shown in Fig. 6. In contrast to gold nanospheres, ACFs of polystyrene and silica nanospheres shifted to the long-delay-time side, implying slower diffusion of nanospheres. Besides, at laser power above 10 mW, the ACF of polystyrene and silica nanospheres appeared to consist of more than one diffusion time constant so the ACF shape changed from single exponential decay. The long-delay-time part of the ACF indicated that some particles in the sample were diffusing slower than the others. Because silica and polystyrene show little absorption at 532 nm, the absorption cross sections of them are almost zero at the wavelength. Therefore we can neglect the absorption force here and laser heating. In addition, such non-metallic materials does not possess strong polarizability, so that their scattering cross sections are also negligible. Eventually we can consider only U_{trap}, indicating that the laser tapping force acts on and stabilizes the particles by the incident laser. This also results in the slower diffusion time with increasing the input laser power. At moment, we cannot discuss the reasons why the diffusion time jump above 10 mW irradiation in both silica and polystyrene and why the ACF curves shows two component at higher laser power irradiation. However, we safely propose that the laser trapping dynamics can be traced by Rayleigh scattering correlation spectroscopy in the case of non-absorbing nanoparticles/molecules without using two lasers for laser trapping and DLS because the both roles can be achieved by the single laser as we demonstrated here.

Downloaded From: http://proceedings.spiedigitallibrary.org/ on 04/27/2014 Terms of Use: http://spiedl.org/terms

4. SUMMARY

We have examined excitation laser power and wavelength dependence on microscopic motions of nanoparticles in suspension on the basis of Rayleigh scattering correlation microspectroscopy. It was clearly found that the diffusion constant of gold nanoparticles decreased with increasing excitation laser power at the excitation wavelength of higher absorption cross section. This behavior was explained in terms of a coupling between laser trapping by the scattering excitation laser itself and laser heating of the particle. In the case of non-absorbing materials, silica and polystyrene, the excitation power dependence can be ascribed only to the laser trapping. This means, when we study molecule/nanomaterials assembling dynamics, for example laser trapping crystallization as we demonstrated, under laser trapping by microscopic DLS, it is not necessary to introduce two lasers for laser trapping and DLS independently, because the scattering excitation laser can be used as the trapping laser simultaneously. On the other hand, in the case of highly thermal conductive material such as metal, the scattering excitation wavelength should be carefully selected to avoid laser heating of particles and following heat dissipation to the surrounding. Recently, laser trapping of metallic nanoparticles with ultrashort pulse laser have been demonstrated[28,29], showing suppression of the heat dissipation. This indicates that ultrashort pulse excitation of DLS can be considered from the viewpoint of the hydrodynamic study of metallic nanoparticles. As mentioned above, DLS can be widespread application in many fields including biological systems, intercellular protein dynamics, reaction kinetics, and so forth compared with FCS because it does not rely on fluorescence tagging technique and/or fluorephore. However, we have demonstrated that the excitation laser itself can act as a trapping laser. We propose that further and detailed examination of the experimental parameters DLS is required depending on the target material, then fruitful investigation will be achieved.

5. REFERENCES

[1] Ashkin, A., “Optical trapping and manipulation of neutral particles using lasers,” Proc. Natl. Acad. Sci. 94(10), 4853-4860(1997).

[2] Neuman, K. C. and Block, S. M., “Optical trapping,” Rev. Sci. Instrum. 75(9), 2787-2809(2004).

[3] Grier, D. G., “A revolution in optical manipulation,” Nature 424(6950), 810-816(2003).

[4] Yoshikawa, H., Matsui, T. and Masuhara, H., “Reversible assembly of gold nanoparticles confined in an optical microcage,” Phys Rev E 70(6), 061406-061411(2004).

[5] Hosokawa, C., Yoshikawa, H. and Masuhara, H., “Cluster formation of nanoparticles in an optical trap studied by fluorescence correlation spectroscopy,” Phys. Rev. E 72, 021408(2005).

[6] Borowicz, P., Hotta, J., Sasaki, K. and Masuhara, H., “Chemical and optical mechanism of microparticle formation of poly(N-vinylcarbazole) in N,N-dimethylformamide by photon pressure of a focused near-infrared laser beam,” J Phys Chem B 102(11), 1896-1901(1998).

[7] Smith, T. A., Hotta, J., Sasaki, K., Masuhara, H. and Itoh, Y., “Photon pressure-induced association of nanometer-sized polymer chains in solution,” J Phys Chem B 103(10), 1660-1663(1999).

[8] Masuo, S., Yoshikawa, H., Nothofer, H. G., Grimsdale, A. C., Scherf, U., Mullen, K. and Masuhara, H., “Assembling and orientation of polyfluorenes in solution controlled by a focused near-infrared laser beam,” J Phys Chem B 109(15), 6917-6921(2005).

Downloaded From: http://proceedings.spiedigitallibrary.org/ on 04/27/2014 Terms of Use: http://spiedl.org/terms

[9] Nabetani, Y., Yoshikawa, H., Grimsdale, A. C., Mullen, K. and Masuhara, H., "Laser deposition of polymer micro- and nanoassembly from solution using focused near-infrared laser beam," Jpn. J. Appl. Phys., 46(1), 449-454(2007).

[10] Tanaka, Y., Yoshikawa, H., Asahi, T. and Masuhara, H., "Laser microfixation of highly ordered J aggregates on a glass substrate," Appl. Phys. Lett. 91(4), 041102-4(2007).

[11] Sugiyama, T., Adachi, T. and Masuhara, H., "Crystallization of glycine by photon pressure of a focused CW laser beam," Chem. Lett. 36(12), 1480-1481 (2007).

[12] Sugiyama, T., Adachi, T. and Masuhara, H., "Crystal Growth of Glycine Controlled by a Focused CW Near-infrared Laser Beam," Chem. Lett. 38(5), 482-483 (2009).

[13] Yuyama, K., Rungsimanon, T., Sugiyama, T. and Masuhara, H., "Selective Fabrication of α-and γ-Polymorphs of Glycine by Intense Polarized Continuous Wave Laser Beams," Cryst. Growth Des. 12(5), 2427-2434(2012).

[14] Hosokawa, C., Yoshikawa, H. and Masuhara, H., "Optical assembling dynamics of individual polymer nanospheres investigated by single-particle fluorescence detection," Phys Rev E 70(6), 061410(2004).

[15] Zhang, Y. and Gu, C., "Optical trapping and light-induced agglomeration of gold nanoparticle aggregates," Phys. Rev. B 73(16), 165405(2006).

[16] Liu, Z.-W., Hung, W.-H., Aykol, M., Valley, D. and Cronin, S. B., "Optical manipulation of plasmonic nanoparticles, bubble formation and patterning of SERS aggregates," Nanotech. 21(10), 105304(2010).

[17] Kuyper, C. L., Fujimoto, B. S., Zhao, Y., Schiro, P. G. and Chiu, D. T., "Accurate sizing of nanoparticles using confocal correlation spectroscopy," J. Phys. Chem. B 110(48), 24433-24441(2006).

[18] Magde, D., Elson, E. and Webb, W. W., "Thermodynamic fluctuations in a reacting system: measurement by fluorescence correlation spectroscopy," Phys. Rev. Lett. 29(11), 705-708(1972).

[19] Eigen, M. and Rigler, R., "Sorting single molecules - Application to diagnostics and evolutionary biotechnology," Proc. Natl. Acad. Sci. 91(13), 5740-5747(1994).

[20] Webb, W. W., "Fluorescence correlation spectroscopy: inception, biophysical experimentations, and prospectus," Appl. Opt. 40(24), 3969-3983(2001).

[21] Hosokawa, C., Yoshikawa, H. and Masuhara, H., "Enhancement of biased diffusion of dye-doped nanoparticles by simultaneous irradiation with resonance and nonresonance laser beams," Jpn. J. Appl. Phys. 16, L453-L456(2006).

[22] Ito, S., Sugiyama, T., Toitani, N., Katayama, G. and Miyasaka, H., "Application of fluorescence correlation spectroscopy to the measurement of local temperature in solutions under optical trapping condition," J. Phys. Chem. B 111(9), 2365-2371(2007).

[23] Shen, Y.R., [The Principles of Nonlinear Optics], Wiley, NY, 366 (1984).

[24] Uwada, T., Sugiyama, T. and Masuhara, H., "Wide-field Rayleigh scattering imaging and spectroscopy of gold nanoparticles in heavy water under laser trapping,, J. Photochem. Photobiol. A: Chem. 221, 187-193 (2011).

[25] Johnson, P. B. and Christy, R. W., "Optical constants of the noble metals," Phys. Rev. B 6(12), 4370-4379 (1972).

[26] Seol, Y., Carpenter, A. E. and Perkins, T. T., "Gold nanoparticles: enhanced optical trapping and sensitivity coupled with significant heating," Opt. Lett. 31(16), 2429-2431(2006).

[27] Keblinski, P., Cahill, D. G., Bodapati, A., Sullivan, C. R. and Taton, T. A., "Limits of localized heating by electromagnetically excited nanoparticles," J. Appl. Phys. 100, 054305(2006).

[28] Jiang, Y.-Q., Narushima, T. and Okamoto, H., "Nonlinear optical effects in trapping nanoparticles with femtosecond pulses," Nat. Phys. 6(12), 1005-1009(2010).

[29] Usman, A., Chiang, W.-Y. and Masuhara, H., "Optical trapping and polarization-controlled scattering of dielectric spherical nanoparticles by femtosecond laser pulses," J. Photochem. Photobiol. A: Chem. 234(SI), 83-90(2012).

Downloaded From: http://proceedings.spiedigitallibrary.org/ on 04/27/2014 Terms of Use: http://spiedl.org/terms